

## NEUTRON OPTICS USING NON-PERFECT CRYSTALS

A.K. Freund

Institut Max von Laue-Paul Langevin,  
B.P. 156, F-38042 Grenoble Cedex, France.

### 1. Introduction

What may be the relation between *neutron optics using non-perfect crystals* and the topic of this workshop which is *imaging processes and coherence in physics*, and what is the difference to *perfect crystal neutron optics*? The term *neutron optics* seems to be rather ill-defined because optics is dealing with light waves or photons and not with neutrons which interact in a fundamentally different way with matter. However, as has been outlined in other papers of this workshop, several principles discovered in optics can be applied also to the description of phenomena occurring at the scattering of X-rays, neutrons and electrons. The present paper deals with the application of *focusing principles* to neutron scattering techniques by the use of imperfect crystals. The aim of these methods is not to create a direct image of the microscopic structure of the sample studied like in microscopy but to concentrate the neutron beam on the sample in order to gain intensity at the expense of angular divergence. Such methods are important because neutron sources are much weaker than X-ray or laser sources and the samples studied are in most cases much smaller than typical neutron beam cross-sections. In addition to this focusing in real space the term *focusing* will be extended also to *reciprocal space* and thereby to instrumental resolution which affects directly the imaging process. The imaging process itself is *indirect* and consists in the reconstruction of atomic positions and motions by means of a Fourier transform using patterns of elastically and inelastically scattered neutron intensities. The sharper the lines in these patterns the better works the imaging process. In the following the principles of geometrical focusing will be given rather than the physics done with neutron scattering and the experimental details for which the literature cited below should be consulted. For completeness, the existence of *time focusing* in neutron scattering techniques must be mentioned; a detailed description of these methods is, however, beyond the scope of this paper.

Despite the fact that focusing principles are known from optics since a long time ago and that they have been applied to experimental methods in several fields of research such as X-ray diffraction, electron scattering and particle accelerators, it took a relatively long time before focusing techniques were proposed for neutron scattering instrumentation. The *Bragg optics* discussed by DACHS and STEHR (1962), JAGDZINSKI (1968), EGERT and DACHS (1970) and DACHS (1970) extended X-ray focusing methods (CAUCHOIS, 1932; JOHANSSON, 1933) to neutron diffraction taking into account

the larger penetration depth of neutrons in curved crystals. MAIER-LEIBNITZ (1967, 1970, 1972) replaced the curved crystals by lamellar systems and proposed several new methods. Since then, much work has been done on theoretical analysis as well as on the real efficiency of focusing systems, and more recently the actual state of focusing neutron monochromators and analysers and their applications has been discussed extensively (AXMANN, 1978).

## 2. Some Words about Neutron Scattering Experiments

In this section a short account is given of the parameters defining a neutron experiment and of the devices used in neutron scattering instrumentation which may be chosen as focusing elements in the beam geometry. More detailed descriptions are to be found in appropriate textbooks (BACON, 1975; KOSTORZ, 1979). Fig. 1 shows a flowchart of a neutron scattering experiment taken from FREUND and FORSYTH (1979). The properties of the neutron beam emerging from a thermal neutron source (see the paper by Forsyth, this conference) are subsequently adapted by devices defining the incident beam to the experimental conditions required. Similar devices are used for the definition of the beam scattered by the sample before reaching the detector. The

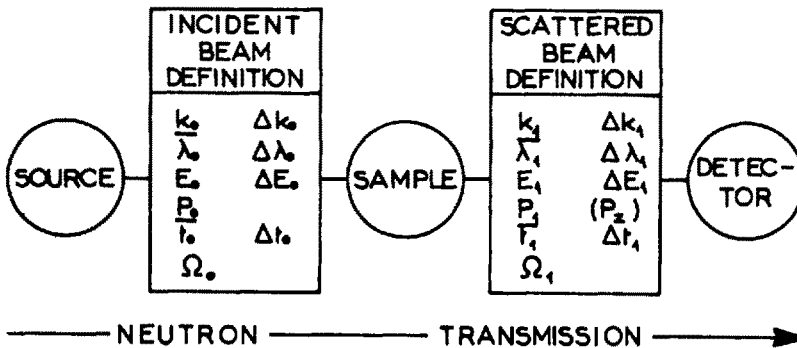
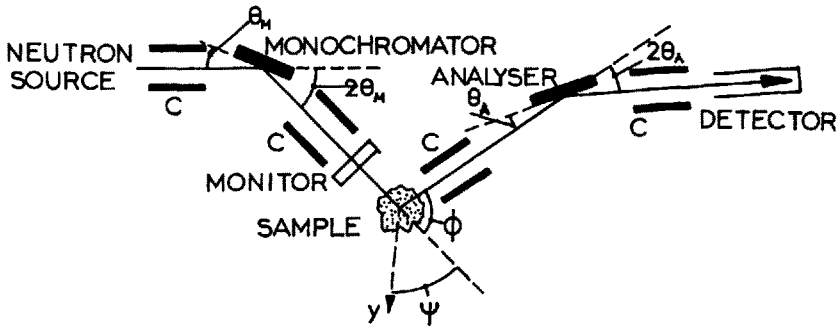


Fig. 1 Schematic diagram of a general neutron scattering experiment

monochromator/polariser determines the incident beam direction confined in a solid angle  $\Omega_0$ , the polarisation  $P_0$ , the neutron energy  $E_0$  and energy spread  $\Delta E$  and thereby the incident wavevector  $k_0$  ( $\pm \Delta k_0$ ). Observation of scattering from the sample is carried out within a solid angle  $\Omega_1$  analysing the polarisation  $P_1$  and the energy  $E_1$  ( $\pm \Delta E_1$ ) corresponding to a wavevector  $k_1$ . Of course, not all the parameters shown in Fig. 1 are independent: a neutron energy  $E$  will have an associated wavelength  $\lambda$ . The choice of description is largely one of convenience for the type of experiment involved, but it may also depend on the choice of the defining device. As already mentioned, this paper will not deal with the time structure of the neutron beam characterised by  $t_0$  and  $t_1$  but with steady state experiments in neutron diffractometry

studying crystal structures by elastic scattering and in three axis spectrometry using inelastic scattering for investigating elementary excitations (phonons, magnons, etc.) in condensed matter.

A typical beam geometry of a triple axis crystal spectrometer is sketched in Fig. 2. A monoenergetic beam of neutrons is obtained by Bragg reflection from the mono-



**Fig. 2** Schematic illustration of a three-axis spectrometer for inelastic neutron scattering experiments

chromator crystal. Its intensity is measured by the monitor just before the sample crystal the orientation of which is specified by the angle  $\psi$  between a crystal axis  $y$  and the incident beam direction. The energy of the neutrons scattered inelastically by the sample at an angle  $\phi$  is determined by an analyser crystal reflecting the beam in direction of the detector. Collimators, diaphragms or slits denoted by  $C$  may be inserted to limit the various neutron beams. At elastic scattering experiments on diffractometers there is in general no need for an analyser crystal except for the elimination of background intensity, and the detector is placed at the position of the analyser. In this case, Bragg scattering from the sample crystal is observed and the angle  $\phi$  in Fig. 2 is replaced by  $2\theta_S$  whereas  $\psi$  becomes  $\pi/2 - \theta_S$  and the axis  $y$  is parallel to the diffraction vector  $\tau$  associated to the set of reflecting lattice planes in the sample. The angles  $\theta_M$ ,  $\theta_S$  and  $\theta_A$  are the Bragg angles of the monochromator, the sample and the analyser crystal, respectively.

The elements defining the beam geometry in Fig. 2 which may be involved in focusing are the monochromator and the analyser crystal and to some extent also the collimators. Focusing microguides based on the principle of total reflection which may also polarise the neutron beam permit to produce a convergent beam (see FREUND and EORSYTH, 1979). Without mentioning details of these devices we focus our attention on the monochromator and the analyser which are imperfect crystals because perfect crystals have a much too narrow width of reflection compared to typical neutron beam divergences. In fact, the widths  $\beta_M$  and  $\beta_A$  of the diffraction curves characterising the degree of imperfection of these crystals should be about equal to  $\alpha_0$ ,  $\alpha_1$ ,  $\alpha_2$  and  $\alpha_3$  being the collimations of the neutron beams before and after the monochromator and before and after the analyser

crystal, respectively. This is the result of an intensity-resolution optimisation (see e.g. MAIER-LEIBNITZ, 1967; DORNER, 1972). The crystal imperfections or dislocations leading to a broadening of the diffraction profiles are generated by plastic deformation of initially nearly perfect crystals.

The diffraction process in imperfect crystals and in particular in crystals used for monochromating and analysing purposes is described by kinematical theory including secondary extinction (ZACHARIASEN, 1945; BACON, 1975; FREUND and FORSYTH, 1979). In the frame of this theory the imperfect crystal with its complicated defect structure is replaced by the so-called *mosaic model* consisting of a composite of small crystal blocks the angular orientation of which are not exactly the same but follow a Gaussian distribution function about a mean orientation. The individual blocks in this composite similar to a brick wall scatter neutrons independently so that the scattered *intensities* will be summed up instead of *amplitudes* in the perfect crystal case. The width of the angular distribution is called the *mosaic spread*  $\eta$  of the imperfect crystal and gives rise to a width  $\beta$  of the neutron diffraction profile recorded from such a crystal. The relation between  $\eta$  and  $\beta$  depends on neutron wavelength and is such that  $\beta \approx \eta$ .

In order to give a schematic illustration of the diffraction conditions and of the influence of beam divergence and mosaic spread on resolution, it is convenient to use the *reciprocal or momentum space* which is obtained by a Fourier transform of real space. The difference between reciprocal and momentum space is just a factor  $2\pi$  in the length of the vectors in Fig. 3 where the diffraction conditions are shown using Ewald's construction projected onto the scattering plane. This is a geometrical construction of Bragg's law given by

$$2d \sin \Theta = \lambda \quad (1a)$$

which can be written as

$$\underline{k}_1 - \underline{k}_0 = 2\pi \underline{\tau} \quad (1b)$$

where  $d$  is the interplanar spacing of the reflecting set of lattice planes,  $\Theta$  is the Bragg angle,  $\lambda$  the neutron wavelength,  $\underline{k}_1$  and  $\underline{k}_0$  the reflected and incident neutron wavevectors such that  $|\underline{k}_1| = |\underline{k}_0| = 2\pi/\lambda$ , and  $\underline{\tau}$  the reciprocal lattice vector or diffraction vector.

The width  $\beta$  of the imperfect crystal diffraction curve is represented in Fig. 3 by a smearing of the reciprocal lattice point corresponding to an angular domain of reflection. The above construction will be used later on in section 4. An account of the *intensity* diffracted by different kinds of *mosaic crystals* has been given by FREUND (1978). For the moment, the discussion returns to real space.

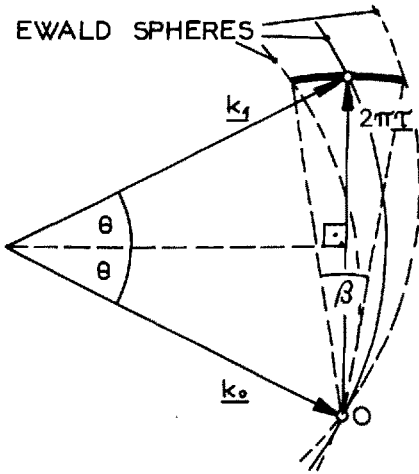


Fig. 3. Diffraction in momentum space of a parallel and monochromatic beam by a non-perfect crystal

### 3. Focusing in Real Space

Focusing in real space consists in concentrating a large neutron beam onto the sample and this can take place in two planes. Focusing in the scattering plane, also called *horizontal focusing* because usually the neutron beam path lies in a horizontal plane, affects directly the resolution whereas *vertical focusing* has practically no influence on the definition of neutron energies or wavevectors. In both cases, curved single crystals or composite crystal systems are used which serve simultaneously as monochromators of the incoming white neutron beam produced by the reactor. An ideal thin crystal bent to a radius  $R$  acts exactly like a mirror with the focal length

$$f_h = (R \sin\theta)/2 \quad (2)$$

in the case of horizontal focusing and

$$f_v = R/(2 \sin\theta) \quad (3)$$

in the case of vertical focusing.

#### 3.1. Horizontal focusing

The neutron beam path in horizontal focusing is shown in Fig. 4. A crystal is bent elastically or plastically to a radius  $R=ON$  and its surface is shaped by grinding such that it has a curvature of  $r = R/2 = OM = MN$ . Any ray emerging from the source and passing through a slit  $S$  positioned at the point  $C$  on the Johansson circle  $J$  will be reflected by the crystal surface onto point  $C'$  which is also on  $J$ .

If a parallel neutron beam is to be focused, for instance when replacing the slit  $S$  by a neutron guide tube or a collimator  $K$  any ray parallel to  $OC$  is converging to the point  $D$  on the focal circle  $F$  defined by Eq. (2). As can be seen from Fig. 4, no change of the Bragg angle is involved in the first case and the focusing is monochromatic.

In the second case, however, the white and nearly parallel beam is focused non-monochromatically and the wavelength reflected depends on the direction of the secondary ray, *i.e.* after reflection from the crystal surface. In both cases the penetration depth of the neutrons in the crystal increases the size of the focal spot as well as the width of the wavelength spread reflected (see the ray CB). This effect is not very large because the crystal thickness is at least two orders of magnitude smaller than the radius of curvature. It is, however, non negligible. On the other hand, aberration effects can be neglected when replacing the Johansson monochromator by a simply bent crystal of the Johann type (JOHANN; 1931). A practical example of horizontal focusing in real space is shown in Fig. 5.

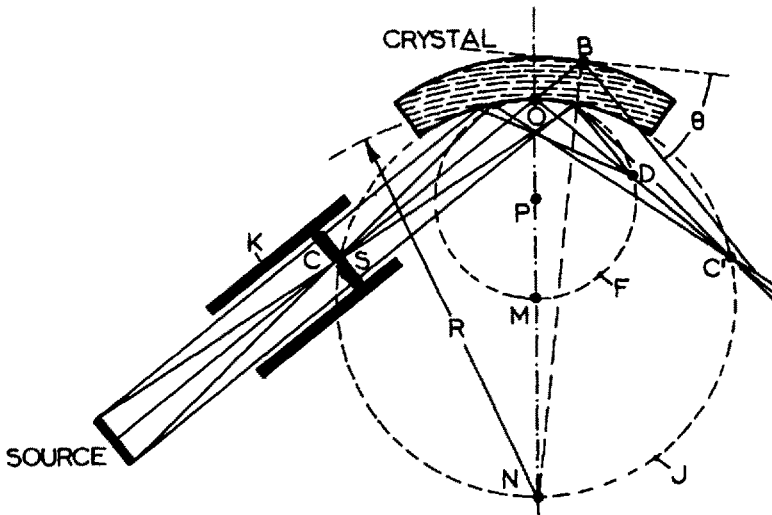


Fig. 4. Horizontal focusing in real space

### 3.2. Vertical focusing

The ray geometry of vertical focusing is sketched in Fig. 6 for again both a divergent and a parallel beam. A crystal is curved cylindrically about an axis lying in the scattering plane LOA. Since the linear dimensions of the crystal are usually small relative to  $R$ , the radius of curvature, aberration may be neglected and the classical formula for hollow mirrors may be used for the projection of the rays onto the plane AOB containing the optical axis OA. This leads to the following relation

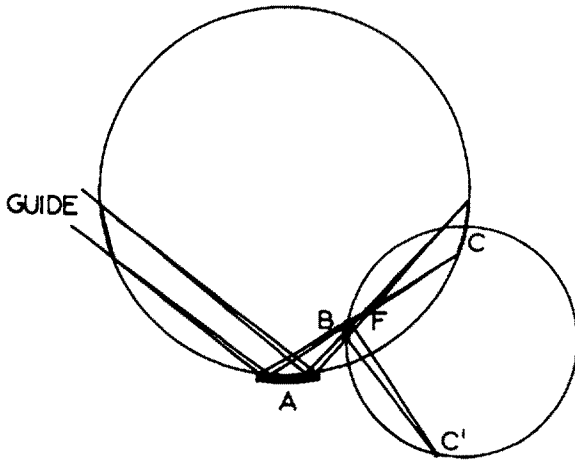


Fig. 5. Guinier geometry on a neutron guide tube. The rays reflected by crystal A meet at F, those scattered at the sample B meet at C'. (From DACHS, 1970)

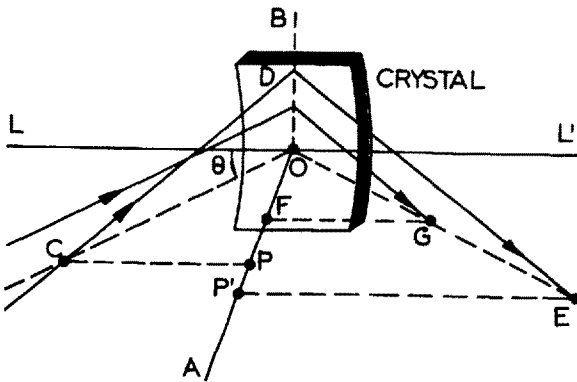


Fig. 6. Vertical focusing in real space. (After RISTE, 1970)

for a point source at C

$$1/OE + 1/OC = (2\sin\theta)/R = 1/f_v \quad (4)$$

and for a parallel beam ( $OC \rightarrow \infty$ )

$$OG = R/(2\sin\theta) = f_v \quad (5)$$

Similar equations can be derived also for horizontal focusing by replacing  $f_v$  by  $f_h$ . As vertical focusing does practically not affect resolution, its application is straightforward and has become very popular. A more detailed analysis of the gain in intensity which can be reached including crystal mosaic spread and beam divergence

has been carried out by Currat (1973). In particular at neutron guide tubes, high gain factors can be reached (FREUND et al., 1978, 1979).

#### 4. Focusing in Reciprocal Space

The possibility of focusing in reciprocal or momentum space arises because the instrumental resolution functions are ellipsoids in three-dimensional reciprocal space for elastic scattering experiments and in a four-dimensional space (energy  $\omega$  and three components of wavevector transfer  $\underline{Q}$ ) for inelastic scattering, with typically a large ratio between the length of its major and minor axes. The orientation of this ellipsoid with respect to the reciprocal space volume defined by the sample (elastic scattering) and to the dispersion relation of the sample crystal (inelastic scattering) determines, together with the scan mode, beam divergence and monochromator mosaic spread, the degree of focusing which can be obtained on neutron diffractometers and three axis spectrometers. These focusing possibilities are rather limited when using flat crystals but may be considerably extended by means of curved monochromators and analysers in particular if the curvature can be made tunable allowing the experimentalist to optimise the experimental conditions by manipulating the resolution function.

The condition for Bragg scattering can be sketched in reciprocal space by the well-known Ewald construction which is represented by Fig. 3 in section 2 of this paper. A slightly modified version of this geometrical construction is represented in Fig. 7 showing diffraction of a divergent white neutron beam by a mosaic crystal monochromator. Shape, size and orientation of the volume in momentum space selected out of the white beam depends not only on the Bragg angle  $\theta_M$  of the monochromator but also on the beam divergence  $\alpha_0$  and on the mosaic spread  $\beta$  of the imperfect monochromator crystal.

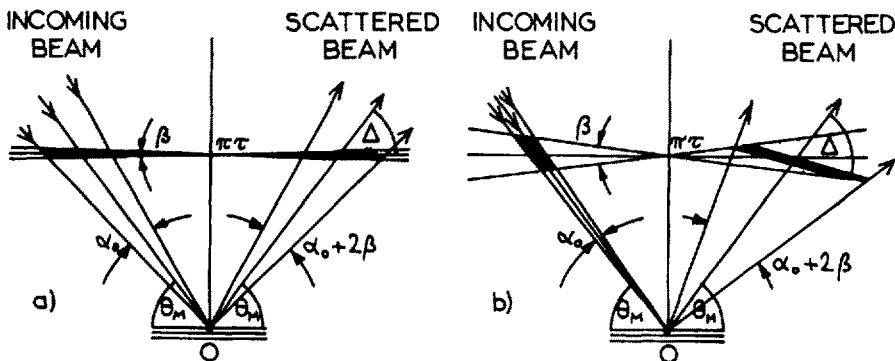


Fig. 7. Selection of momentum space volume by an imperfect crystal, a)  $\alpha_0 > 2\beta$ ;  
b)  $\alpha_0 < 2\beta$



In addition, the momentum spread  $\Delta k = k_{\max} - k_{\min}$  may be further limited by the beam divergence  $\alpha_1$  after reflection.  $\Delta$  gives the orientation of the volume in momentum space,  $\tau_M = 2\pi/d$  is the reciprocal lattice vector and 0 is the origin of the reciprocal lattice. For  $\alpha_0 > 2\beta$  one obtains  $\Delta = \theta_M$  whereas for  $\alpha_0 < 2\beta$  the angle  $\Delta$  is given by the relation  $\text{tg}\Delta = 2\text{tg}\theta_M$ . The relative momentum or wavelength spreads associated  $\Delta k/k = \Delta\lambda/\lambda$  are given by  $\beta \text{ctg}\theta_M$  in the first and  $\alpha_0 \text{ctg}\Delta$  in the second case, respectively (KALUS and DORNER, 1973).

The volume in k-space impinging on the sample crystal is subsequently scanned by e.g. turning the sample through its Bragg position in a diffraction experiment, and the width  $w$  of the intensity profile recorded is described by the relation

$$w = [\alpha_0^2(1 - \text{tg}\theta_S/\text{tg}\theta_M)^2 + \beta^2(2 - \text{tg}\theta_S/\text{tg}\theta_M)^2 + \gamma^2]^{1/2} \quad (6)$$

where  $\theta_S$  is the Bragg angle and  $\gamma$  the mosaic spread of the sample crystal, respectively. The function  $w(\theta_S)$  is called the resolution curve of the diffractometer if  $\gamma$  is negligible. Gaussian distributions of  $\alpha_0$ ,  $\beta$  and  $\gamma$  are assumed for simplicity. For  $\alpha_0 > 2\beta$  the curve  $w(\theta_S)$  has a minimum at  $\theta_S = \theta_M$  which is called the *dispersion-free arrangement* in a double-crystal diffractometer. This minimum is shifted to the position  $\text{tg}\theta_S = 2\text{tg}\theta_M$  for the condition  $\alpha_0 < 2\beta$ . By drawing the sample diffraction conditions in Figs. 7a and 7b and rotating its reciprocal lattice vector about 0 one can see that the minimum of the resolution curve corresponds to scanning the momentum volumes selected by the monochromator crystal in a direction perpendicular to its large axis. *This is called focusing in momentum space.*

The possibility of varying the distance  $L$  between monochromator and sample and the use of a monochromator crystal with tunable radius of curvature allows the adaptation of the experimental conditions to the requirements defined by the sample such that focusing both in real and reciprocal space may be achieved simultaneously leading to an intensity gain without loss in resolution. Fig. 8 shows diffraction from a curved crystal both in real and in momentum space. The orientation of the volume element defined by a curved monochromator crystal is described by the angle  $\Delta$  and related to the beam geometry by

$$\text{tg}\Delta = \text{tg}\theta_M/[1 - L/(R\sin\theta_M)] \quad (7)$$

By choosing  $L$  and  $R$  it is possible to adjust  $\Delta$  in a predetermined way.

The *thickness*  $\Delta k$  of the momentum element parallel to the vector  $\underline{k}$  is determined by the crystal mosaic spread  $\beta$  and the crystal thickness  $T$ . By the use of nearly perfect crystals one can match  $\Delta k$  to the resolution required choosing the thickness according to

$$\Delta k/k = (T\text{ctg}^2\theta_M)/R \quad (8)$$

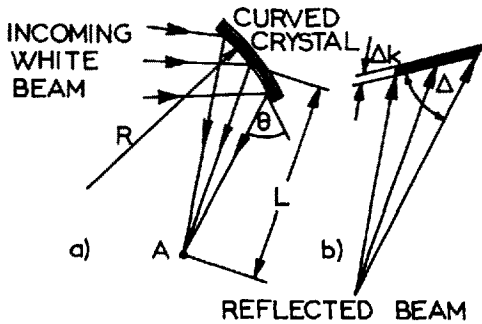


Fig. 8. Bragg scattering from a curved single crystal in (a) real space and (b) momentum space :  $R$  = radius of curvature;  $L$  = distance between single crystal and sample

This equation holds for thermally curved crystals (KALUS *et al.*, 1973) and plastically bent monochromators (EGERT, 1974; HOHLWEIN, 1975). In the case of elastically bent crystals Eq. (8) becomes

$$\Delta k/k = T(\text{ctg}^2 \Theta_M - \mu)/R \quad (9)$$

where  $\mu$  is Poisson's ratio, and if a sandwich of many thin crystals each of thickness  $t$  is used (KALUS, 1975; FREY, 1971, 1974, 1975)

$$\Delta k/k = nt(\text{ctg}^2 \Theta_M - \mu/n)/R \quad (10)$$

where  $n$  is the number of crystals. The dimension of the momentum element perpendicular to  $\underline{k}$  is given by slits or collimators defining the beam geometry.

A somewhat different approach to focusing in reciprocal and real space has been proposed by MAIER-LEIBNITZ (1967) and followed up by RUSTICHELLI (1969) and BOEUF and RUSTICHELLI (1973). A composite monochromator system (Fig. 9) is made up of a set of crystalline lamellas each of which is inclined to the following one by the width  $\beta$  of its diffraction pattern. If the crystal is imperfect,  $\beta$  corresponds to about the mosaic spread, if it is perfect  $\beta$  is given by the so-called Darwin width. In the general case the crystals are cut asymmetrically ("Fankuchen cut") where the degree of asymmetry is determined by the focusing requirements. Such a system as well as the bent crystals mentioned above have several advantages when compared to a classical flat mosaic crystal monochromator. The Gaussian mosaic distribution is replaced by a nearly rectangular distribution leading to a sharper definition of the wavelength and angular spread of the neutron beam impinging on the sample. The momentum distribution in the neutron beam reflected by the composite system shown in Fig. 9 (real space) is sketched in Fig. 10a (momentum space). If  $\beta$  is small as it is the case in typical applications, the thickness  $\Delta k$  of the momentum space element is determined by the divergence  $\alpha_0$  of the primary

white neutron beam according to

$$\Delta k/k = (\alpha_0/2) \text{ctg} \theta_M \quad (11)$$

whereas its dimension parallel to  $\underline{k}$  depends on the number of lamellas. The focusing is non-monochromatic and thus the wavelength of a reflected ray depends on its direction.

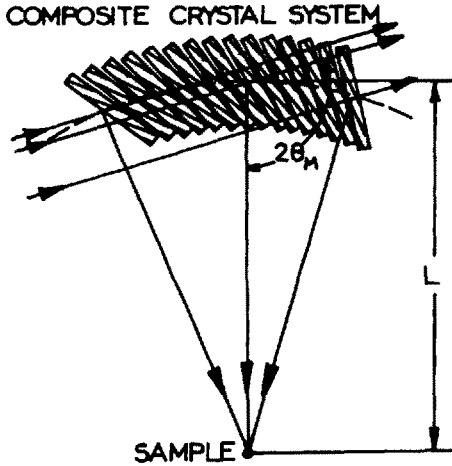


Fig. 9. Schematic representation of the selection of neutron energy by a neutron monochromator system consisting of plane crystalline lamellas. (After MAIER-LEIBNITZ, 1967).

There is a possibility of producing *monochromatic focusing* by a composite system when using crystals with a gradient of lattice spacing or lamellas which have just slightly different lattice parameters. Normally, this should be in the order of some percent in  $\Delta a/a$ . Such a system reflects a neutron beam with a momentum space distribution shown in Fig. 10b and can be considered as a *monochromatising neutron lens*. A composite system of crystals with different lattice spacings has been described recently by BOEUF *et. al.* (1978).

Parallel to the development of such systems also the theory for neutron diffraction by perfect crystals had to be modified for slightly distorted crystals (KLAR and RUSTICHELLI, 1973; ALBERTINI *et. al.*, 1976 a,b). Detailed descriptions of these sophisticated systems and theories are beyond the scope of this paper despite their interest from the "optical" point of view. Comparison between experiment and model calculations have given good agreement (ALBERTINI *et. al.*, 1977) but the application of nearly perfect crystals to neutron monochromatisation is still limited last but not least because of practical problems arising at the production of composite systems.

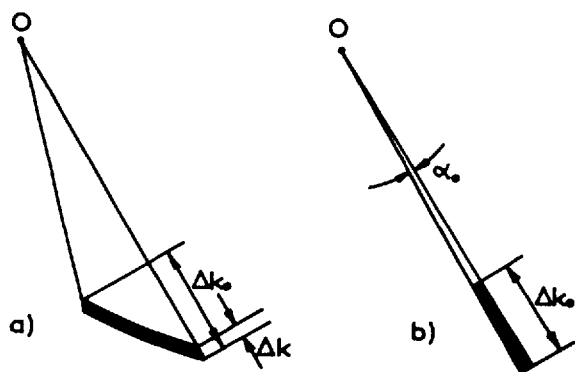


Fig. 10. Momentum space distribution in a neutron beam reflected by (a) a system without and (b) a system with a gradient in lattice spacing. (After RUSTICHELLI, 1970)

### 5. Some Examples of Focusing Methods in Neutron Scattering Techniques

A so-called *modified Laue method* has been proposed by MAIER-LEIBNITZ (1967) for a considerable gain of measuring time in crystal structure analysis. A bent or composite monochromator crystal reflects a large wavelength band on a stationary sample and excites a large number of reciprocal lattice points simultaneously. Whereas in the classical Laue method all higher order reflections fall in the same direction and cannot be separated the new Laue method allows to measure these reflections independently since the focusing is non-monochromatic (Fig. 11). This technique has to use a multidetector or a film (KLAR, 1973; THOMAS, 1972; HOHLWEIN, 1977).

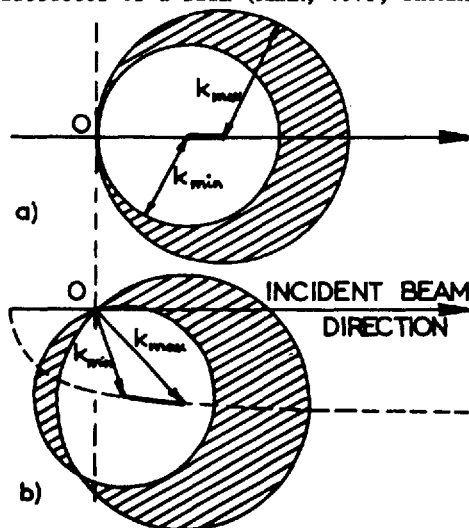


Fig. 11. Laue method in reciprocal space and Ewald spheres corresponding to  $k_{\min}$  and  $k_{\max}$ . (a) Classical method (b) new Laue method. All reciprocal lattice points lying in the hatched region contribute to the Laue diagram.

With increasing momentum space volume of the neutron beam impinging on the sample also the background intensity will become more important. This background which is mostly arising from inelastic scattering processes could be eliminated by a second composite system of crystalline lamellas mounted between the sample and the

detector (Fig. 12).

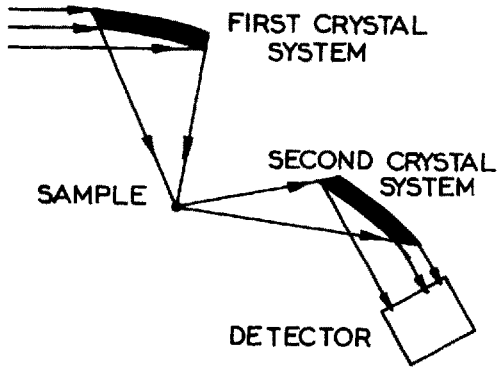


Fig. 12. Focusing method for the measurement of many reflections excluding inelastic scattering. (After MAIER-LEIBNITZ, 1967)

The geometrical considerations which are applied to neutron monochromators can also be extended to *focusing analysers* in order to gain intensity i.e. measuring time. An analyser crystal with variable radius of curvature has been developed for three-axis spectrometers by SCHERM *et. al.* (1977) and some applications of this device are described by SCHERM and WAGNER (1977). The focusing geometry is shown in Fig. 13 in real and reciprocal space. A curved analyser is used to turn the resolution ellipsoid in  $Q$ - $\omega$ -space by varying the radius of curvature and the analyser-detector distance  $L_D$ . To each element of the multidetector is associated a volume element in  $Q$ - $\omega$ -space designed by the numbering in Fig. 13. Three cases are presented :

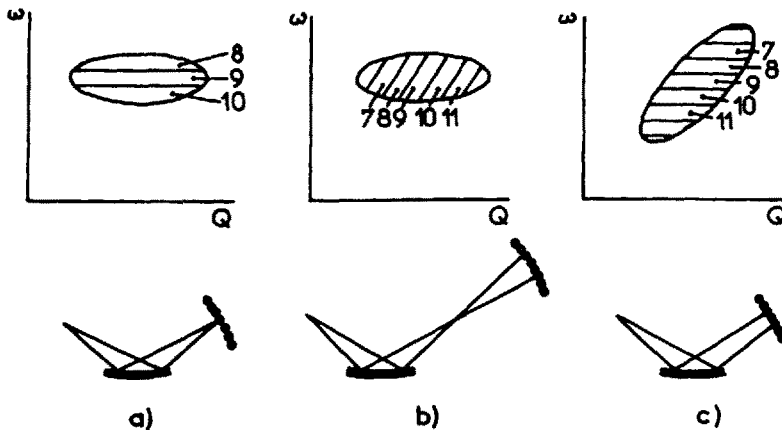


Fig. 13. Triple axis spectrometry using a curved analyser and a multidetector. (After SCHERM and WAGNER, 1977).

- (a)  $R = R^x$  and  $L_D = 2f_h = L_A$   
 (b)  $E = R^x$  and  $L_D \gg L_A$   
 (c)  $R > R^x$  and  $L_D = L_A$

where  $L_A$  is the sample-analyser distance and  $R^x = L_A \cdot d \cdot k / \pi$ . The collimators between sample, analyser and detector have been removed (*c.f.* Fig. 2). Fig. 13 demonstrates the different kinds of possibilities arising when choosing focusing geometry with variable  $R$  and  $L_D$ . Also flat samples can be used in these methods.

The angular precision of crystal orientation is somewhat relaxed at the construction of composite perfect or nearly perfect crystal analysers in inelastic neutron spectrometers working at Bragg angles close to  $90^\circ$ . Several thousands of Si and  $\text{CaF}_2$  nearly perfect crystals were glued on curved surfaces covering several square metres and serve as focusing analysers in the high-resolution backscattering instruments IN10 and IN13 at the Institut Laue-Langevin (BIRR *et. al.*, 1971).

Some other possible applications are discussed by FREY (1978), GRIMM (1978), KALUS (1978) and AXMANN *et. al.* (1978). In conclusion, it can be said that focusing techniques in neutron scattering are still in the developing stage except vertical focusing. Whereas principles are clear, some problems still arise at the practical construction of high-precision composite crystal systems with variable curvature. Efforts are being made at the Institut Laue-Langevin and at other reactor stations in order to solve this problem. It is important to have the possibility of tuning the curvature of monochromators and analysers not only because the radius of curvature is energy or wavelength dependent but also for operating an instrument in the classical *flat-crystal and collimator mode* if this appears to be preferable (availability of large samples, danger of multiple scattering etc.). Further developments of focusing methods are expected in connection with the construction of pulsed neutron sources and multidetector systems.

## References

- Albertini, G., Boeuf, A., Cesini, G., Mazkedian, S., Melone, S., and Rustichelli, F. (1976a). *Acta Cryst.* A32, 863-868  
 Albertini, G., Boeuf, A., Mazkedian, S., Melone, S., Rozzi, V., and Rustichelli, F. (1976b). *J. Appl. Cryst.* 10, 118-122  
 Albertini, G., Boeuf, A., Klar, B., Lagomarsino, S., Mazkedian, S., Melone, S., Puliti, P., and Rustichelli, F. (1977). *Phys. Stat. Sol.* A44  
 Axmann, A. (1978). Proceedings of the workshop on Fokussierende Neutronenmonochromator und Analysatoranordnungen, Hahn-Meitner-Institut, Berlin. HMI Report B273  
 Axmann, A., Kasper, F., and Dachs, H. (1978). In : Axmann (1978), p. 168  
 Bacon, G.E. (1975). *Neutron Diffraction*, third edition. Clarendon Press, Oxford  
 Birr, M., Heidemann, A., and Alefeld B. (1971). *Nucl. Instr. and Methods.* 95, 435  
 Boeuf, A., and Rustichelli, F. (1973). *Nucl. Instr. and Methods* 107, 429-435  
 Boeuf, A., Detorbet, P., Escoffier, A., Hustache, R., Lagomarsino, S., Rennert, A., and Rustichelli, F. (1978). *Nucl. Instr. and Methods* 152, 415-421  
 Cauchois, Y. (1932). *J. Phys.* (7) 3, 320  
 Currat, R. (1973). *Nucl. Instr. and Methods* 107, 21-28  
 Dachs, H. (1970). *J. Appl. Cryst.* 3, 220-224  
 Dachs, H., and Stehr, H. (1962). *Z. Kristallogr. Kristallgeom. Kristallphys. Kristallchem.* 117, 135-145

- Dorner, B. (1972). Acta Cryst. A28, 319-327
- Egert, G. (1974). J. Appl. Cryst. 7, 564
- Egert, G., and Dachs, H. (1970). J. Appl. Cryst. 3, 214-220.
- Freund, A. (1978). In : Axmann (1978), p.1.
- Freund, A., and Forsyth, J.B. (1979). In : Neutron Scattering in Materials Science (G. Kostorz, editor). Chapter X. Vol. 15 of the series A Treatise on Materials Science and Technology (H. Herman, editor). Academic Press, New York, in press
- Freund, A., Hewat, A.W., Scherm, R., and Zeyen, C. (1977). Report 77FR115S, Institut Laue-Langevin, Grenoble
- Freund, A., Hustache, R., and Zeyen, C. (1977). To be submitted to Nucl. Instr. and Methods
- Frey, F. (1971). Nucl. Instr. and Methods 96, 471-473
- Frey, F. (1974). Nucl. Instr. and Methods 115, 277-284
- Frey, F. (1975). Nucl. Instr. and Methods 125, 9-17
- Frey, F. (1978). In : Axmann (1978), p. 54
- Grimm, H. (1978). In : Axmann (1978), p. 73
- Hohlwein, D. (1975). J. Appl. Cryst. 8, 465-468
- Hohlwein, D. (1977). Acta Cryst. A33, 649
- Jagodzinski, H. (1968). Acta Cryst. B24, 19
- Johann, H.H. (1931). Z. Phys. 69, 185
- Johansson, T. (1933). Z. Phys. 82, 507
- Kalus, J. (1975). J. Appl. Cryst. 8, 361-364
- Kalus, J., and Dorner, B. (1973). Acta Cryst. A29, 526-528
- Kalus, J., Gobert, G., and Schedler, E. (1973). J. Phys. E6, 488-492
- Klar, B. (1973). Ph. D. Thesis, Universität Hamburg
- Klar, B., and Rustichelli, F. (1973) Nuovo Cimento B13, 249-271
- Kostorz, G. (1979). Neutron Scattering in Materials Science. Vol. 15 of the series A Treatise on Materials Science and Technology (H. Herman, editor). Academic Press, New York, in press
- Maier-Leibnitz, H. (1967). Ann. Acad. Sci. Fenn., Phys. Ser. A6, 267, 1-17
- Maier-Leibnitz, H. (1970). In : Some Lectures on Neutron Physics, Report JINR, p. 183 Dubna
- Maier-Leibnitz, H. (1972). In : Inelastic Neutron Scattering, p. 681. IAEA, Vienna
- Riste, T. (1970). Nucl. Instr. and Methods 86, 1-4
- Rustichelli, F. (1969). Nucl. Instr. and Methods 74, 219-223
- Rustichelli, F. (1970). Nucl. Instr. and Methods 83, 124-130
- Scherm, R., and Wagner, V. (1977). In : Inelastic Neutron Scattering, p. 1. IAEA, Vienna
- Scherm, R., Dolling, G., Ritter, R., Schedler, E., Teuchert, W., and Wagner, V. (1977) Nucl. Instr. and Methods 143, 77-85
- Thomas, P. (1972). J. Appl. Cryst. 5, 78-83
- Zachariasen, W.H. (1945). Theory of X-Ray Diffraction in Crystals. Wiley, New York.